

Finite Larmor radius effects on the coupled trapped electron and ion temperature gradient modes

I. Sandberg^{a)}

Department of Electrical and Computer Engineering, National Technical University of Athens, GR-157 73, Association Euratom-Hellenic Republic, Athens, Greece

H. Isliker

Department of Physics, Aristotle University of Thessaloniki, GR-541 24, Association Euratom-Hellenic Republic, Thessaloniki, Greece

V. P. Pavlenko

Department of Astronomy and Space Physics, Uppsala University, Box 515, SE-751 20, Euratom-VR Fusion Association, Uppsala, Sweden

(Received 1 May 2007; accepted 16 July 2007; published online 13 September 2007)

The properties of the coupled trapped electron and toroidal ion temperature gradient modes are investigated using the standard reactive fluid model and taking rigorously into account the effects attributed to the ion polarization drift and to the drifts associated with the lowest-order finite ion Larmor radius effects. In the flat density regime, where the coupling between the modes is relatively weak, the properties of the unstable modes are slightly modified through these effects. For the peak density regions, where the coupling of the modes is rather strong, these second-order drifts determine the spectra of the unstable modes near the marginal conditions. © 2007 American Institute of Physics. [DOI: [10.1063/1.2768938](https://doi.org/10.1063/1.2768938)]

I. INTRODUCTION

Low-frequency electrostatic turbulence driven by spatial gradients is believed to be the main source of anomalous transport in magnetically confined fusion plasma.^{1,2} During recent years, a significant number of both theoretical and numerical investigations in plasma dynamics have been focused on the effects related to the development of low-frequency drift-wave instabilities. Particular attention has been paid to the properties of the toroidal ion temperature gradient (ITG) mode³ due to the successful interpretations of various experimental results by means of the dynamics of the ITG mode. However, a significant part of the detected electron heat transport is attributed to the component of plasma turbulence that is driven by the trapped electron modes (TEM),⁴ which are localized in the low-field region of tokamaks.

For the development of the ITG instability, the ion temperature gradient is necessarily to be combined with other effects such as the magnetic curvature, the parallel incompressibility, or the presence of impurity species.⁵ In toroidal magnetic configurations, the instability is mainly driven by the magnetic field curvature⁶ and it is termed toroidal ITG mode instability. In the frame of a collisionless two-fluid model, the explicit threshold of the instability was recently obtained⁷ by taking rigorously into account the effects attributed to the ion polarization drift and to the drifts associated with the lowest-order finite ion Larmor radius (FLR) effects.

It was actually shown that the effects associated with these second-order drifts modify significantly the properties of the toroidal ITG modes. For the peak density regions, for

instance, the instability threshold may decrease significantly, and the associated marginal unstable modes acquire finite wavelengths. On the other hand, the excitation of the TEM instability requires the presence of trapped electrons combined with the electron pressure gradient in toroidal plasma. When the driving term is the background density gradient, the induced unstable mode is referred to as the pure TE mode, and when the driving term is the electron temperature gradient, the induced mode can be termed the ETG-driven TE mode.

A series of experimental data shows the importance of the toroidal ITG and the TEM instabilities for the levels of the observed transport of energy. ITG and TE modes can coexist depending on the local plasma parameters and, as will be shown here, on the finite ion Larmor radius effects. Recently, a series of investigations has focused on the combined effects of trapped electrons on the ITG modes,⁸ on the generation of TEM turbulence,⁹ and on the excitation of the associated zonal flows.¹⁰ The derivation of a general model to describe these modes can be obtained either from a low-frequency expansion of the general fluid equations¹¹ based on the drift velocity ordering, or by using as a starting point the nonlinear gyrokinetic equations.¹²

In this work, we investigate the properties of the coupled system of ITG-TE modes, motivated through the fact that in the regions of peak plasma density, (a) the coupling between the modes is rather strong¹⁰ and (b) the drift effects attributed to ion polarization and to FLR effects are crucial for the stability of the toroidal ITG mode.⁷

Landau effects and dissipative effects will be omitted. A relative discussion related with these issues can be found in Ref. 8. It is claimed that when the fraction of TE is increased, the frequency shift in the direction of higher nega-

^{a)}Electronic mail: sandberg@central.ntua.gr

tive frequencies of the ITG modes can possibly give less Landau damping. Another possible destabilizing mechanism attributed to dissipative effects is the contribution by the TE density perturbations through dissipation effects such as collisions or magnetic–drift resonances.¹³

In what follows, we adopt and analyze the so-called reactive two-fluid model¹⁴ and focus on the coupling properties of the modes that arise due to second-order drift effects that become significant in peak density regions. In Sec. II, the system of the basic equations is presented, the linearization of which leads to the derivation of the coupled dispersion relation of ITG-TE modes. In Sec. III, we present some characteristic numerical solutions of the coupled dispersion relation for various plasma parameters. The results of a numerical simulation of the nonlinear evolution of the coupled ITG-TE mode is briefly presented. A discussion and a summary of the major findings follows in Sec. IV.

II. COUPLED ITG-TEM FLUID EQUATIONS

The advanced reactive fluid model by Weiland¹⁴ for the coupled system of ITG-TE modes is adopted and investigated by keeping rigorously the terms attributed to the polarization drift and to drifts associated with the lowest-order FLR effects. In the 2D slab geometry, adopted here, the curved magnetic field is modeled by $\mathbf{B}=B_0\mathbf{b}$, where the magnitude and the direction of the field are given by $B_0(x)=B_0(1-x/R)$ and $\mathbf{b}=\hat{z}-(z/R)\hat{x}$, respectively, and R is the radius of curvature of the magnetic field lines. The considered plasma inhomogeneities are along the \hat{x} axis, while the direction of plasma drifts is along the \hat{y} axis. Effects attributed to parallel ion dynamics, magnetic shear, Landau damping, or finite beta are omitted.

In the low-frequency limit $\omega \ll \omega_{ci}$, the ion polarization drift and the drifts associated with FLR effects can be considered small compared to the electric and the diamagnetic drifts. This is the usual drift velocity ordering and allows to express the perpendicular component of the ion velocity by a perturbation expansion. In this limit, the linearized continuity and temperature equations for the trapped electrons and the ions can be written in the following normalized form,¹⁰ respectively:

$$\frac{\partial n_{et}}{\partial t} + f_t \frac{\partial \phi}{\partial y} + \epsilon_n \frac{\partial}{\partial y} [-f_t \phi + n_{et} + f_t T_{et}] = 0, \quad (1)$$

$$\frac{\partial T_{et}}{\partial t} + \frac{5}{3} \epsilon_n \frac{\partial T_{et}}{\partial y} + \left(\eta_e - \frac{2}{3} \right) \frac{\partial \phi}{\partial y} - \frac{2}{3 f_t} \frac{\partial n_{et}}{\partial t} = 0, \quad (2)$$

$$\begin{aligned} \frac{\partial n_i}{\partial t} - \left[\frac{\partial}{\partial t} - \tau(1 + \eta_i) \frac{\partial}{\partial y} \right] \nabla_{\perp}^2 \phi + \frac{\partial \phi}{\partial y} \\ - \epsilon_n \frac{\partial}{\partial y} [\phi + \tau(n_i + T_i)] = 0, \end{aligned} \quad (3)$$

$$\frac{\partial T_i}{\partial t} - \frac{5}{3} \tau \epsilon_n \frac{\partial T_i}{\partial y} + \left(\eta_i - \frac{2}{3} \right) \frac{\partial \phi}{\partial y} - \frac{2}{3} \frac{\partial n_i}{\partial t} = 0. \quad (4)$$

The structure of the terms in Eqs. (1)–(3) and (2)–(4) are naturally quite similar to each other. However, this similarity is essentially broken by the term proportional to $\nabla_{\perp}^2 \phi$ in Eq. (3), which is attributed to the ion polarization drift terms including lowest-order FLR effects. Indeed, there is a strong similarity between the polarization drift caused by the time variation of the perturbed electric field and the low-order finite Larmor radius drift, which is due to the space variation of electric field.¹⁴

The system of equations (1)–(4) gets closed by assuming quasineutral oscillations, $n_i = n_e = n_{et} + n_{ef}$, and a Boltzmann density response (i.e., $\phi = n_{ef}$) for the untrapped electron population. Here, ϕ represents the perturbed potential and T_j , n_j are the perturbed temperature and density of plasma species j , where $j=i, et, ef$ stands for ions, trapped, and free electrons, respectively. The length and the time scales have been normalized with respect to $\rho_s = c_s / \omega_{ci}$ and L_n / c_s , respectively, where $c_s^2 = T_e / m_i$, $\omega_{ci} = e B_0 / m_i c$, and $L_g^{-1} = -d \ln g(x) / dx$. The electrostatic potential has been normalized as $\phi = e \delta \phi / T_e L_n / \rho_s$, the perturbed density as $n_j = \delta n_j / n_0 L_n / \rho_s$, and the perturbed ion temperature as $T_j = \delta T_j / T_{j0} L_n / \rho_s$. Furthermore, the curvature of the magnetic field lines R and the ion temperature inhomogeneity scale lengths L_{T_j} are given in terms of the plasma inhomogeneity scale length L_n by $\epsilon_n = 2 L_n / R$ and $\eta_j = L_n / L_{T_j}$, respectively. Lastly, $\tau = T_i / T_e$ denotes the ratio between ion and free-electron temperature and $f_t = n_{et0} / n_0$ is the density ratio of the trapped electrons.

III. LINEAR PROPERTIES OF THE COUPLED DISPERSION EQUATION

Using the usual Fourier expansion for the perturbed quantities, $\tilde{g}(r, t) = \tilde{g} \exp(i \mathbf{k}_{\perp} \cdot \mathbf{r} - i \omega t)$, one may derive the following dispersion equation:

$$\begin{aligned} \frac{\omega}{k_y} (\epsilon_n - 1) + \tau \epsilon_n \left(\eta_i - \frac{7}{3} + \frac{5}{3} \epsilon_n \right) + k_{\perp}^2 \left[\frac{\omega}{k_y} + \tau(1 + \eta_i) \right] \left(\frac{\omega}{k_y} + \frac{5}{3} \tau \epsilon_n \right) \\ + f_t \frac{\omega}{k_y} (1 - \epsilon_n) + \epsilon_n \left(\eta_e - \frac{7}{3} + \frac{5}{3} \epsilon_n \right) \\ \frac{\omega^2}{k_y^2} + \frac{10}{3} \frac{\omega}{k_y} \tau \epsilon_n + \frac{5}{3} \tau^2 \epsilon_n^2 \\ \frac{\omega^2}{k_y^2} - \frac{10}{3} \frac{\omega}{k_y} \epsilon_n + \frac{5}{3} \epsilon_n^2 \end{aligned} + 1 - f_t = 0. \quad (5)$$

Here, $k = k_{\perp} = (k_x, k_y)$ denotes the perpendicular to the toroidal axis of the magnetic field wave number and ω is the frequency of the mode. The first term in Eq. (5) describes the ion response, the second term the trapped electron response, and the last terms the response of the free electrons. In the appropriate limits, $\tau, T_i, f_t, L_{T_j}, R \rightarrow 0$, one may reproduce the dispersion relation of the electron drift wave, $\omega = k_y / (1 + k_{\perp}^2) > 0$, which propagate in the positive \hat{y} direction.

In the more general case, the dispersion equation (5) describes coupled ITG-TE modes that may coexist depending on the

local plasma parameters R/L_n , R/L_{Te} , R/L_{Ti} , T_i/T_e , and, as will be shown here, on the finite ion Larmor radius effects. In the flat density regime, i.e., $\epsilon_n \sim 1$, the ITG and the TE modes are relatively weakly coupled with each other. For the case of negligible coupling, one may obtain the instability threshold for the toroidal ITG instability in the presence of trapped electrons by simply omitting the response of the trapped electrons. This can be justified only in the case in which the second term in Eq. (5) is small enough compared to the first one. In Eq. (5), the second-order drift effects are represented by the term proportional to k_\perp^2 in the first fractional term of the sum. Working in a similar manner to that in Ref. 7, we keep the terms proportional to k_\perp^2 and after some lengthy calculations we determine the explicit threshold for the development of the ITG instability in the presence of trapped electrons,

$$\eta_{iTh} = \begin{cases} \eta_{iTh1} = \frac{2}{3} + \frac{10}{9} \epsilon_n \tau (1 - f_i) \\ \text{for } \epsilon_n < 1, \text{ and } \epsilon_n > 1 \text{ when } 0 < \tau < \tau_*, \\ \eta_{iTh2} = \eta_{iTh1} + \frac{(\epsilon_n - 1)^2}{4 \epsilon_n \tau (1 - f_i)} \\ \text{for } \epsilon_n \geq 1 \text{ when } \tau > \tau_*, \end{cases} \quad (6)$$

where $\tau_* \equiv \frac{3}{2}(1 - 1/\epsilon_n)/(1 - f_i)$.

The threshold values η_{iTh} as obtained here do not depend on the wave number of the excited mode provided that $k_y \neq 0$. As long as $\eta_i > \eta_{iTh}$, the toroidal ITG instability in the presence of TE is going to be developed. The value of the wave number of the most unstable mode will depend on the plasma parameters including the value of η_i . In the absence of second-order drift effects, the threshold of the instability is given by $\eta_{iTh} = \eta_{iTh2}$ (Ref. 14) and the marginally unstable mode has wave number $k_{m\perp} = 0$. However, as was proved and discussed in Ref. 7, the polarization drift including the FLR effects lowers the instability threshold to $\eta_{iTh} = \eta_{iTh1}$ when (a) $\epsilon_n < 1$ and (b) $\epsilon_n > 1$ provided that $0 < \tau < \tau_*$. The marginally unstable mode in the latter cases has finite wavelength since $k_{m\perp} \neq 0$. As a result, the spectra of the unstable modes $\gamma(k_\perp)$ for conditions above marginal stability range from $0 < k_{\perp+} < k_\perp < k_{\perp-}$, where the values of $k_{\perp\pm}$ have been analytically derived in Ref. 7. This result showed that the polarization drift including the FLR effects is a destabilizing factor in peak density regions, while for large wave numbers it is always stabilizing, as expected.

When the second term in Eq. (5) is large enough compared to the first one, one may omit the effect of the ion perturbations and obtain the instability threshold η_{eTh} for the ETG-driven TE mode,¹⁰

$$\eta_{eTh} = \frac{2}{3} - \frac{\xi}{2} \left(1 - \frac{\epsilon_n}{2} - \frac{1}{2\epsilon_n} \right) + \frac{10}{9} \frac{\epsilon_n}{\xi}, \quad \xi = \frac{f_i}{1 - f_i}. \quad (7)$$

The considered assumptions for the derivation of Eqs. (6) and (7) can be justified when the denominators in Eq. (5) are different by at least one order of magnitude. However, even for weak-coupling conditions, the response of both ions and trapped electrons will influence the properties of the TE and ITG modes, respectively. In what follows, we present

some numerical solutions of the dispersion equation corresponding to different plasma conditions. In all the cases presented below, we restrict our discussion for the most unstable modes, i.e., those with $k_x = 0$ and $k_\perp = k_y$.

A. Pure TE mode

The simplest case is to study the properties of the coupled TE modes by neglecting both electron and ion temperature inhomogeneities ($\eta_{i,e} = 0$) and keeping the ion response term, which includes the ion FLR effects. The numerical solution Eq. (5) in the flat density regime, $\epsilon_n \sim 1$, shows that the pure TE mode propagates in the electron drift direction, i.e., $+\hat{y}$. In contrast, in the peak plasma density regions $\epsilon_n \ll 1$, where the coupling between the ion and the electron response becomes stronger, the pure TEM propagates either in the electron $+\hat{y}$ or in the ion drift direction $-\hat{y}$ depending on its wave number and on the ratio of the temperatures τ .

In Fig. 1, the growth rate of the TE mode is plotted for various values of ϵ_n and τ . It is evident that the TE mode gets more unstable as τ and/or ϵ_n decrease. In Fig. 2, the frequency ω and the growth rate γ of the TE mode are plotted versus $k = k_y$ for different values of τ and fixed the rest plasma parameters. For small wave numbers, the mode propagates in the electron drift direction, and for large wave numbers in the ion drift direction. Decreasing τ , we find that the number of the modes that propagate in the electron drift direction increases and *vice versa*. This is expected as the contribution of the electron drift to the real frequency of the TE mode dominates as the ratio T_i/T_e decreases.

In the absence of second-order drift effects, the dispersion relation obtains the form $\omega/k_y = F(\epsilon_n, \tau, \eta_i, \eta_e, f_i)$ resulting in a nondispersive relation since $\omega \propto k_y$. The existence of a narrow instability region $0 < k_{\perp+} < k_\perp < k_{\perp-}$ (for $\epsilon_n \ll 1$) and the stabilization of the modes (for any ϵ_n) at large wave numbers were found also in Ref. 7 for the case of the pure ITG mode. Obviously, these effects are attributed to the polarization drift and to the drifts associated with FLR effects, which may enhance the electrostatic potential near marginal stability conditions depending on the wave number.

B. The TE-ITG mode

In this subsection, we consider the presence of an ion temperature gradient and investigate the stability and dispersion properties of the coupled ITG and TE modes.

In the weak-coupling limit, $\epsilon_n = 1$, $\tau = 1$, the threshold of the toroidal ITG instability in the absence of trapped electrons is given by $\eta_{iTh} = 1.78$. However, by considering even a tiny fraction of trapped electrons $f_i = 0.067$, we notice a small but remarkable decrease in the value of the threshold to $\eta_{iTh} = 1.70$ according to Eq. (6).

As a case study for the strong-coupling limit, we keep the parameters $\epsilon_n = 0.2$, $\tau = 10$, and $f_i = 0.2$ and we choose three different values for η_i 's. For $\eta_i = 0$, the unstable pure TE mode appears as expected, but for $\eta_i = 1$ we notice that the TE instability gets totally suppressed by the ion temperature inhomogeneity. Further increase to $\eta_i = 2.35$ leads to the reappearance of an unstable mode driven now by the ion

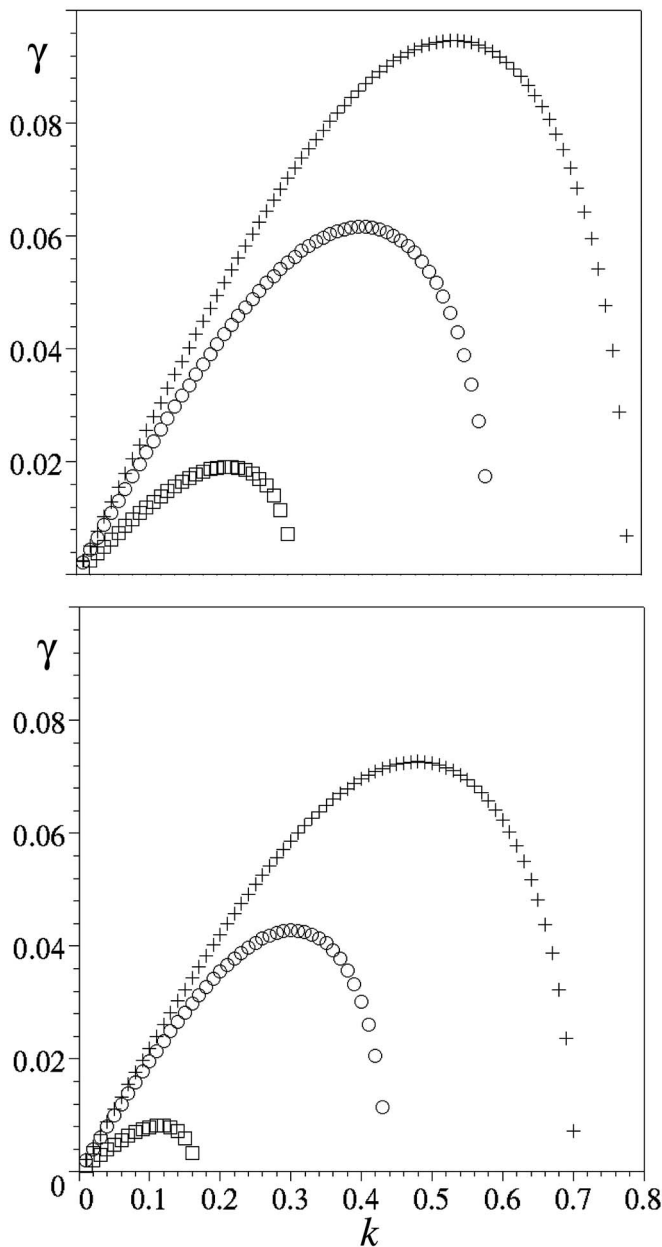


FIG. 1. The spectra of the pure TE mode for different plasma parameters. In the upper panel, $\epsilon_n=0.6$ (crosses), $\epsilon_n=0.7$ (circles), $\epsilon_n=0.8$ (boxes) for $\tau=0.7$ and $f_i=0.2$. In the lower panel, $\tau=0.5$ (crosses), $\tau=1$ (circles), $\tau=1.5$ (boxes) for $\epsilon_n=0.7$ and $f_i=0.2$. It is evident that an increase of ϵ_n and/or τ leads to the stabilization of the TE mode.

temperature gradient. This ITG mode appears for η_i much smaller compared to the threshold of the pure toroidal ITG instability (i.e., $\eta_{iTh}=2.89$ for $f_i=0$) and smaller than the threshold obtained when taking into account the fraction of the trapped electrons ($\eta_{iTh}=2.44$) but neglecting the TE response according to Eq. (6). In Fig. 3, we present a case in which the ITG instability threshold is numerically determined from Eq. (5). It is shown that the instability develops for smaller values of η_i than those presented in Eq. (6). This leads us to the conclusion that both the presence and the response of trapped electrons decrease the η_i threshold for the development of the toroidal ITG instability.

In Fig. 4, we have plotted the growth rate of the TE-ITG

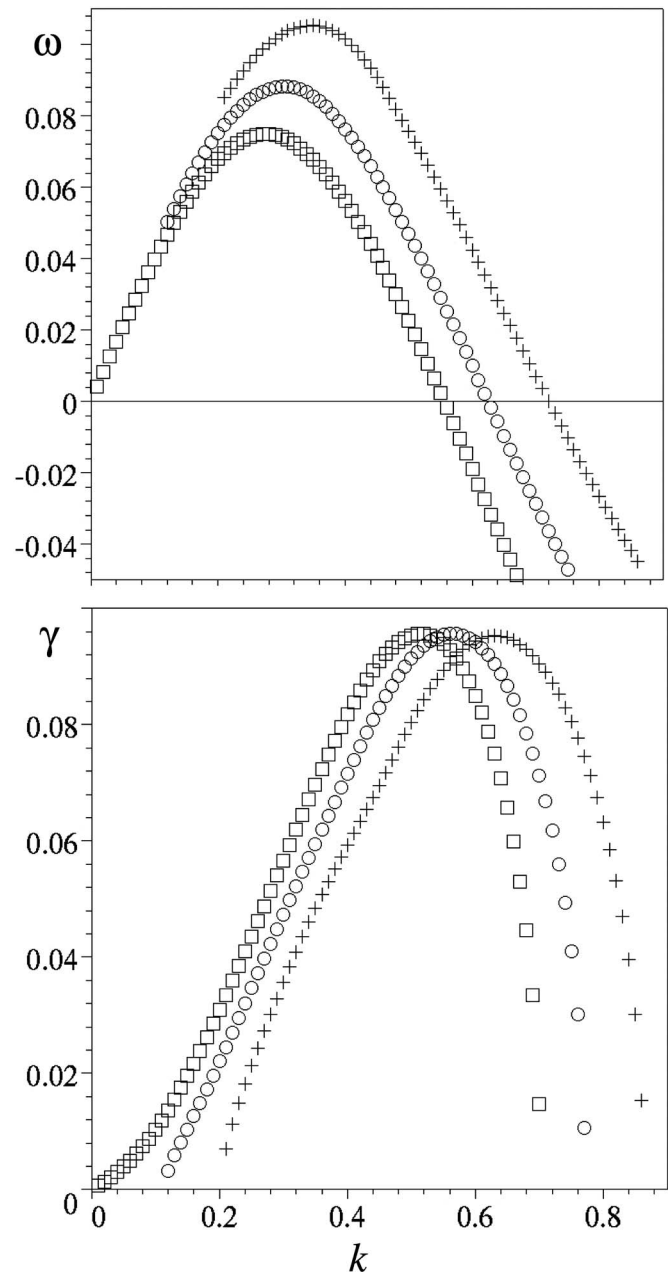


FIG. 2. The frequency and the growth rate of the pure TE mode. The chosen values for the plasma parameters are $\epsilon_n=0.1$, $f_i=0.2$, and $\tau=2$ (circles), $\tau=2.5$ (crosses), $\tau=3$ (boxes).

coupled mode for $\epsilon_n=0.3$, $\tau=1$, $\eta_i=0.95$, and $f_i=0.15$. The unstable spectrum shows a single unstable mode with two distinct peaks attributed to the TE and the ITG characteristics, respectively. The mode propagates toward the electron drift direction for large wavelengths, and toward the ion drift direction for smaller wavelengths. Remarkably, a stable zone appears for a narrow region of wave numbers as shown in Fig. 4 for $k_{\perp} \approx 0.5$. As explained in Sec. III A, all these features are attributed to the second-order drifts, including the FLR effects, which modify significantly the spectra especially near the marginal conditions. In the absence of these effects, all the dispersion curves would be linear, i.e., $\omega \propto k_y$, with a constant of the slope that determines the stability of the mode, equal to ω/k_y independent of the wave number.

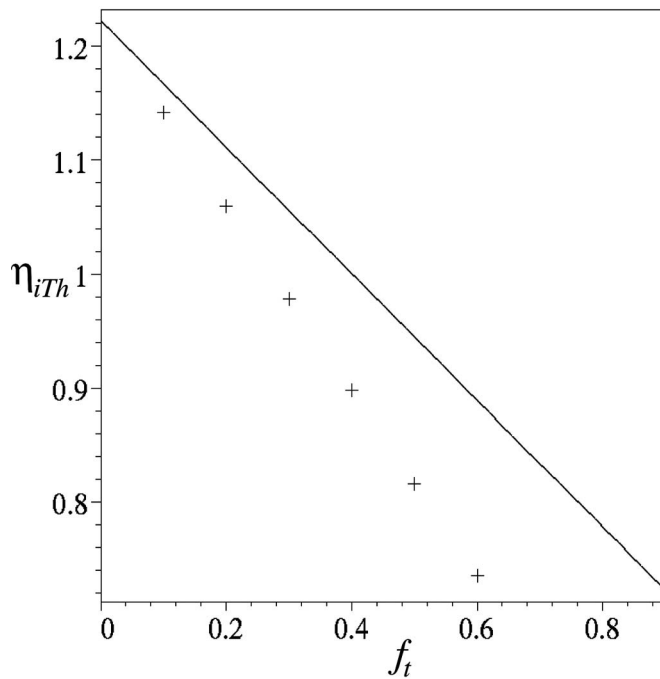


FIG. 3. The dependence of the ITG instability threshold on the fraction and the response of the trapped electrons. The solid line represents the approximated solution given by Eq. (6)—which omits the TE response—while the crossed points represent the threshold values as numerically obtained. The chosen values for the plasma parameters here are $\epsilon_n=0.5$, $\eta_e=0$, and $\tau=1$.

C. The ETG-driven TE-ITG mode

The trapped electron modes can be driven unstable by the electron temperature gradient. In the presence of an electron temperature gradient, the numerical solution of the dispersion equation in the weak-coupling limit gives two unstable solutions. The first solution corresponds to the ETG-driven TE mode and the second one to the toroidal ITG mode. From the corresponding numerical solutions, we note that an increase of η_i leads to a decrease of the growth rate of the ETG-driven TE mode, and an increase of η_e leads to a decrease of the ITG growth. Thus, we conclude that there is a competitive effect between the temperature gradient driven modes. However, an increase of the ratio of the electron trapped population f_t will lead to a subsequent increase of the growth rates for both modes, as expected. In Fig. 5, the growth rate and the frequencies of the ITG and the ETG-driven TE modes are presented for $\epsilon_n=1$, $\tau=1$, $\eta_i=1.45$, $\eta_e=3$, and $f_t=0.4$, which correspond to a weak-coupling case. The TE mode propagates toward the electron drift direction while the ITG toward the ion drift direction. The stabilization of both modes for large wave numbers is clearly related to ion FLR effects.

In the strong-coupling limit, $\epsilon_n \ll 1$, there exists a single unstable solution with different spectral characteristics depending on the plasma parameters such as the ratio of the temperatures and the temperature gradients. For the marginally unstable case determined by the parameters $\epsilon_n=0.2$, $\tau=1$, $\eta_i=0.9$, $\eta_e=0.7$, and $f_t=0.1$, we present in Fig. 6 the growth rate and the frequency of the single unstable solution versus the wave number. A noticeable feature of the spectra

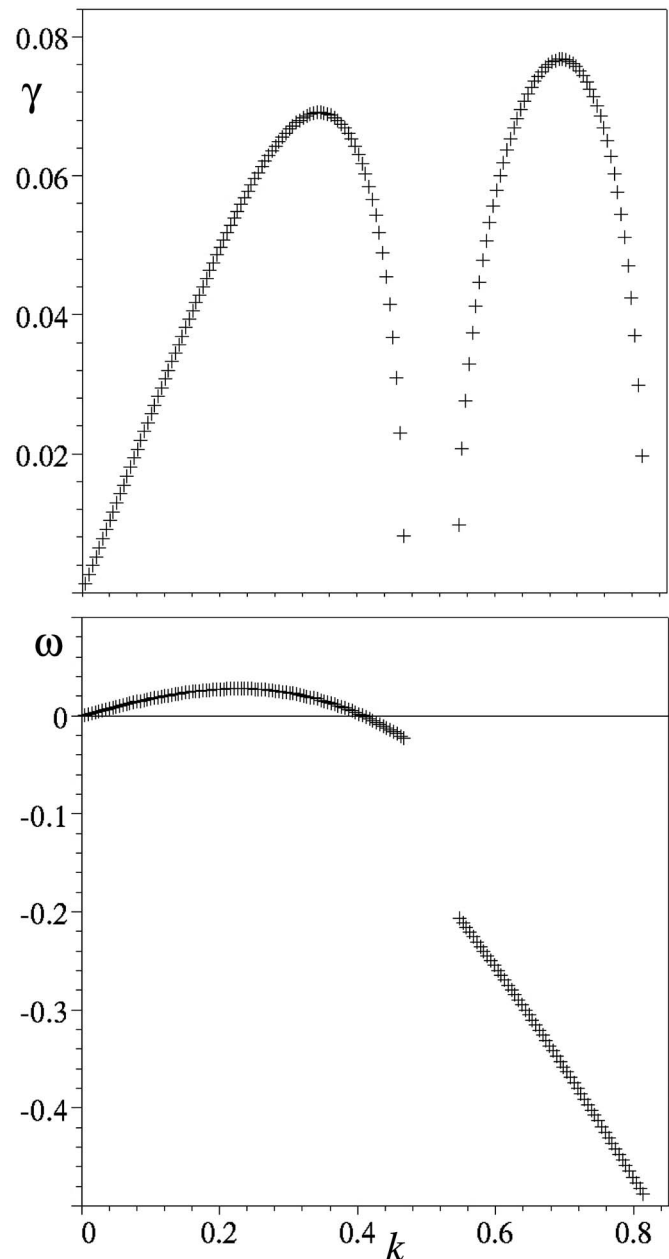


FIG. 4. The growth rate and the frequency of a strongly coupled TE-ITG mode. The chosen values for the plasma parameters are $\epsilon_n=0.3$, $\tau=1$, $\eta_i=0.95$, $\eta_e=0$, and $f_t=0.15$.

for the chosen parameters is the appearance of three different peaks at the spectra. Looking at Fig. 6(b), we can conclude that the peaks at the lowest wave numbers are attributed to the trapped electrons while those at the highest wave number correspond to the ion response. Modifying properly the plasma parameters, we identify the driving mechanism responsible for the appearance of each peak. The peak at the lowest wave number is attributed to the ETG driver, the one at the highest wave numbers is due to the ITG driver, while the one in the middle corresponds to the pure TE mode driven by the density gradient. An increase of η_e leads to the suppression of the peaks attributed to the ITG and the ϵ_n drivers. In order to verify independently these findings, we performed a numerical simulation of the temporal evolution

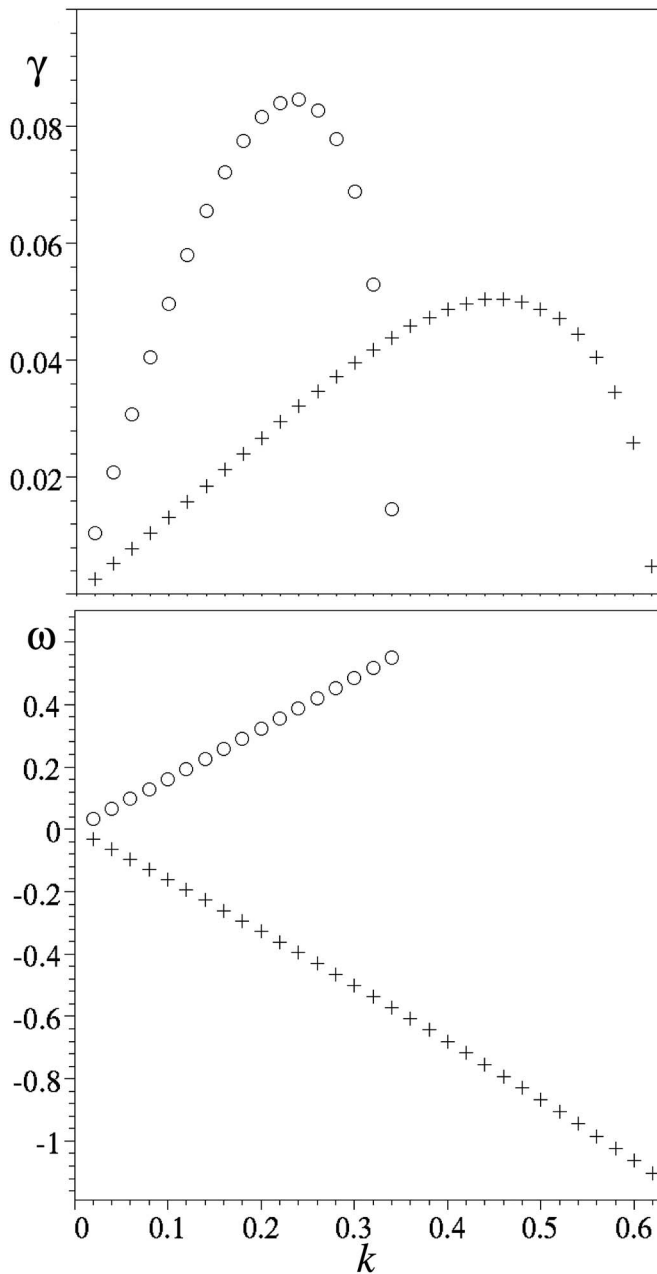


FIG. 5. The growth rate and the frequency of weakly coupled ETG-driven TE and ITG modes. The chosen values for the plasma parameters are $\epsilon_n = 1$, $\tau = 1$, $\eta_i = 1.45$, $\eta_e = 3$, and $f_i = 0.4$. The circles corresponds to the TE mode and the crosses to the ITG mode.

of Eqs. (1)–(4). The obtained 2D spectra were in full agreement with the numerical analysis of the dispersion relation plotted in Fig. 6(a). It becomes evident that in the peak density regions, where the FLR effects become more important, three distinct peaks related to different instability mechanisms may coexist even on slightly different scales. The choice of the particular parameters ($\epsilon_n = 0.2$, $\tau = 1$, $\eta_i = 0.9$, $\eta_e = 0.7$, and $f_i = 0.1$) leads to the clear appearance of these three nonoverlapped peaks revealing that the behavior of the single unstable solution in such conditions—as they are typical in peak density regions—is actually attributed to coupled instability mechanisms.

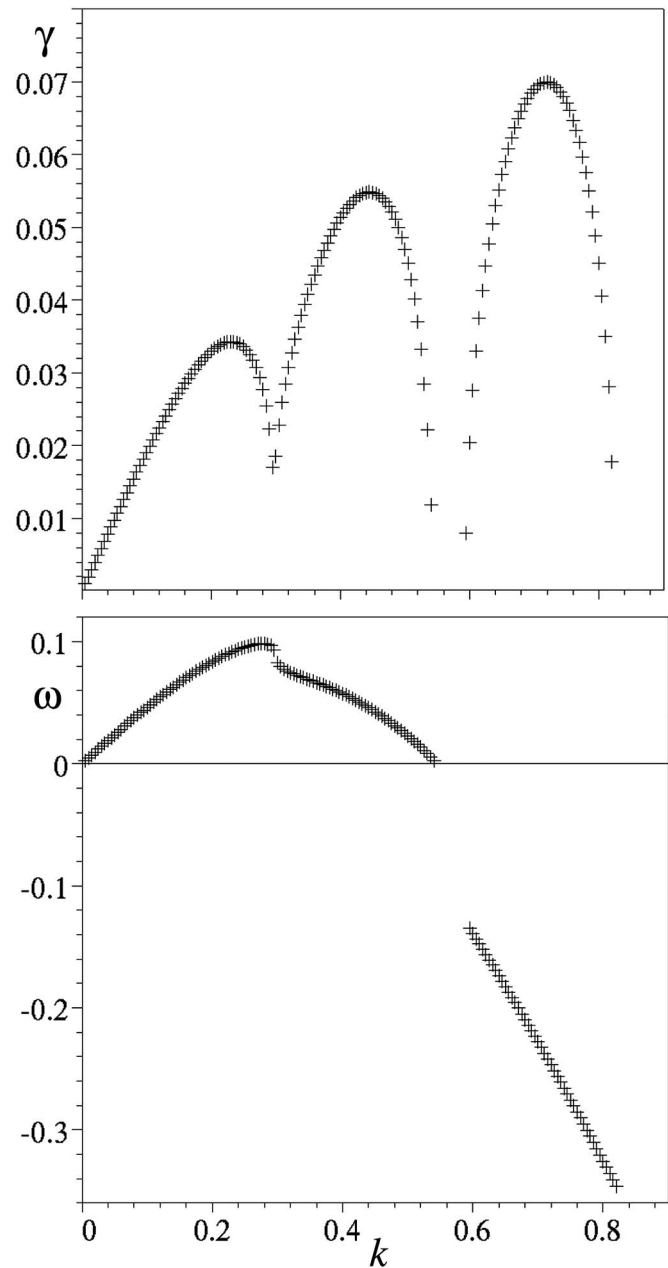


FIG. 6. The growth rate and the frequency of a strongly coupled ETG-driven TE-ITG mode. The chosen values for the plasma parameters are $\epsilon_n = 0.2$, $\tau = 1$, $\eta_i = 0.9$, $\eta_e = 0.7$, and $f_i = 0.1$.

IV. RESULTS AND DISCUSSION

The stability and the dispersion properties of the strongly coupled ITG and TE modes were analytically and numerically investigated on the basis of the reactive two-fluid model. It was shown that in the peak density regions, where the coupling of the modes is rather strong, the ion finite Larmor radius effects affect strongly the stability and dispersion properties of the coupled modes. In the absence of temperature gradients, a pure TE mode appears that is marginally unstable in a finite spectral region with $k_{\perp} \neq 0$, a property that is attributed solely to the second-order drift terms, which include the FLR effects. In the presence of an ion temperature gradient, the unstable spectrum may consist of two coexistent modes (in flat density regions) or of a

single mode that is the result of the strong coupling (in peak density regions) between the TE–ITG modes. TE lower the instability threshold through their dynamics and through their fraction of density.

The presence of an electron temperature gradient leads to an additional driving mechanism responsible for the development of the so called ETG-driven TEM instability. In this case, the marginally unstable spectrum in the peak density plasma regions consists of a single unstable mode, and may exhibit three distinct peaks, each attributed to a different driving mechanism. In conclusion, second-order drifts including ion FLR effects stabilize both TE and ITG modes at small wavelengths, decrease the instability thresholds, and permit the coexistence of different unstable modes in a narrow region of wave numbers.

ACKNOWLEDGMENTS

The authors are thankful to the referee for his constructive criticism, which enabled the improvement of the presented work.

This work was supported under the Contract of Association ERB 5005 CT 99 0100 between the European Atomic Energy Community and the Hellenic Republic. The sponsors do not bear any responsibility for the contents in this work.

¹W. Horton, *Rev. Mod. Phys.* **71**, 735 (1999).

²P. W. Terry, *Rev. Mod. Phys.* **72**, 109 (2000).

³L. I. Rudakov and R. Z. Sagdeev, *Sov. Phys. Dokl.* **6**, 415 (1961).

⁴P. C. Liewer, *Nucl. Fusion* **25**, 543 (2005).

⁵D. Jovanović and W. Horton, *Phys. Plasmas* **2**, 1561 (1995).

⁶B. Coppi and F. Pegoraro, *Nucl. Fusion* **17**, 969 (1977).

⁷I. Sandberg, *Phys. Plasmas* **12**, 050701 (2005).

⁸P. Malinov and F. Zonca, *J. Plasma Phys.* **71**, 301 (2005).

⁹T. Dannert and F. Jenko, *Phys. Plasmas* **12**, 072309 (2005).

¹⁰J. Anderson, H. Nordman, R. Singh, and J. Weiland, *Plasma Phys. Controlled Fusion* **48**, 651 (2006).

¹¹S. I. Braginskii, in *Reviews of Plasma Physics*, edited by M. A. Leontovich (Consultants Bureau, New York, 1965), Vol. 1.

¹²T. Hahm, W. Lee, and A. Brizard, *Phys. Fluids* **31**, 1940 (1988).

¹³C. Z. Cheng, *Nucl. Fusion* **22**, 773 (1982).

¹⁴J. Weiland, *Collective Modes in Inhomogeneous Plasmas*, (IOP Publishing, Bristol, 2000).